REVIEW ARTICLE
https://doi.org/10.1038/s41929-022-00747-w

nature catalysis

Check for updates

Critical enzyme reactions in aromatic catabolism for microbial lignin conversion

Erika Erickson[1,2,6], Alissa Bleem[1,2,6], Eugene Kuatsjah[1,2,6], Allison Z. Werner[1,2,6], Jennifer L. DuBois[3], John E. McGeehan[4], Lindsay D. Eltis[5] ✉ and Gregg T. Beckham[1,2] ✉

The application of microbes to valorize aromatic compounds derived from the abundant plant biopolymer lignin is a rapidly developing area of research that may ultimately enable viable conversion of this recalcitrant and heterogeneous resource to valuable bio-based chemical products. Starting from the three canonical lignin building blocks, which differ in the extent of aromatic ring methoxylation, several common classes of enzymatic reaction occur in the upper pathways of aromatic catabolism to prepare aromatic compounds for assimilation into central carbon metabolism, including aromatic *O*-demethylation, hydroxylation and decarboxylation. These critical enzymatic steps can often be rate-limiting for efficient biological funnelling of aromatic compounds. Here we review the known enzymatic mechanisms for these reactions that are relevant for aerobic aromatic catabolism of lignin-related monomers, highlighting opportunities at the intersection of biochemistry, enzyme engineering and metabolic engineering for applications in the expanding field of microbial lignin valorization.

Lignin is a heterogeneous aromatic plant cell wall biopolymer that is synthesized via radical coupling reactions of three primary monolignols: *p*-coumaryl alcohol (H unit), coniferyl alcohol (G unit) and sinapyl alcohol (S unit) (Fig. 1a)[1]. Given the available reactive centres of the monolignols, the lignin polymer is typically composed of a heterogeneous network linked by C–O and C–C bonds. Recent work has revealed that components beyond the traditional three monolignols can be incorporated into lignin (Fig. 1b), including flavonoids, hydroxystilbenes and hydroxycinnamic amides[2]. In addition, lignin can be covalently linked to hemicellulose and often exhibits pendent hydroxycinnamic acids or benzoic acids, depending on the plant species[2,3]. The resulting polymer has a complex structure that lends rigidity and hydrophobicity to the plant cell wall, facilitating upward growth and water transport, respectively.

The natural abundance of biomass provides promising opportunities for lignin conversion to supply chemical products that are currently derived from fossil-based feedstocks. Indeed, industrial conversion of lignin into value-added products is critical to the viability of a lignocellulosic bioeconomy[4,5]. However, lignin remains under-utilized because its compositional heterogeneity presents challenges for selective depolymerization and upgrading or direct use as a material (Fig. 1a). Although a wide variety of strategies have been pursued with the goal of depolymerizing lignin into monomers and oligomers[6–10], the resulting heterogeneous mixtures of phenolic compounds can require costly separation steps for chemical production. Thus, continued research and innovation is required to realize lignin valorization at scale.

One approach with the potential to overcome the utilization barrier for lignin is biological funnelling, which harnesses microbial metabolic pathways to convert heterogeneous chemical mixtures into a defined product with high atom efficiency[11–19]. Aerobic catabolism of aromatic compounds is particularly well suited to this approach, as these pathways converge on a few central intermediates and are amenable to engineering[20]. In bacteria, this catabolism involves activation of the aryl ring by oxygenation reactions. These reactions occur in upper pathways, so named for their roles in catabolizing a wide variety of aromatic compounds to a small number of shared intermediates. Lower pathways then transform these intermediates to central metabolites[21]. Shared intermediates include catechol, protocatechuate and gallate, three compounds that are subject to ring-opening catalysed by dioxygenases (Fig. 1c)[22,23]. In an alternative aerobic aromatic catabolic strategy, not discussed here, the aromatic ring is activated by coenzyme A (CoA) thioesterification before hydrolytic cleavage[21]. Metabolic engineering efforts, primarily in bacteria that catabolize aromatics aerobically, have converted aromatic substrates in lignin-derived streams to value-added compounds[11,13,15,17–20,24–30]. The ultimate viability of biological funnelling strategies relies on convergent microbial pathways that transform lignin towards target molecules.

In this Review we focus on three key classes of enzymatic reaction that enable the catabolism of lignin-related compounds (referred to hereafter as LRCs) to target products in bacterial hosts. All three classes of reaction activate aromatic compounds for oxidative ring-opening, namely *O*-demethylation, hydroxylation and decarboxylation. Importantly, in the context of effective microbial biocatalysts for lignin valorization, these reactions are increasingly recognized as rate-limiting steps[13,27,29,31–33]. Optimization of these steps through enzyme engineering, metabolic engineering and experimental evolution is coming to the forefront as an exciting and biotechnologically critical application for realizing industrial-scale biological lignin valorization.

Aromatic *O*-demethylation

Catalytic and thermal depolymerization of lignin feedstocks, especially those from angiosperms that are rich in G/S-type lignin units,

[1]Renewable Resources and Enabling Sciences Center, National Renewable Energy Laboratory, Golden, CO, USA. [2]Center for Bioenergy Innovation, Oak Ridge National Laboratory, Oak Ridge, TN, USA. [3]Department of Chemistry and Biochemistry, Montana State University, Bozeman, MT, USA. [4]Centre for Enzyme Innovation, School of Biological Sciences, University of Portsmouth, Portsmouth, UK. [5]Department of Microbiology and Immunology, BioProducts Institute, and the Life Sciences Institute, The University of British Columbia, Vancouver, British Columbia, Canada. [6]These authors contributed equally: Erika Erickson, Alissa Bleem, Eugene Kuatsjah, Allison Z. Werner. ✉e-mail: leltis@mail.ubc.ca; gregg.beckham@nrel.gov

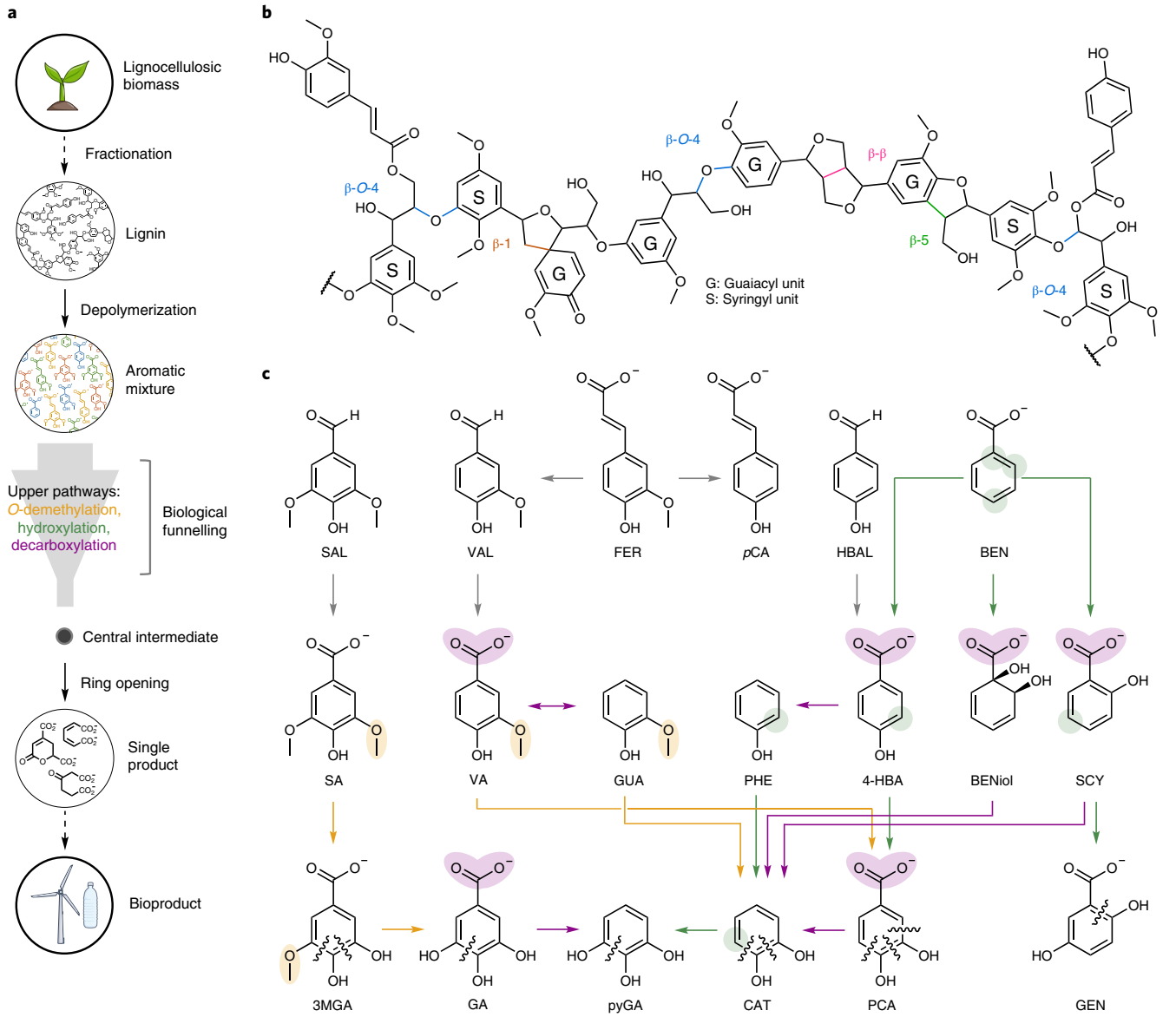

Fig. 1 | Activation of lignin-relevant compounds. a, A generalized lignin valorization process that employs fractionation and depolymerization of lignin to a mixture of compounds, and subsequently biological funnelling to convert the mixture to a single target product, represented here by the examples β-ketoadipate, *cis*,*cis*-muconate and 2-pyrone-4,6-dicarboxylic acid. These compounds can then be utilized in direct replacement chemicals or performance-advantaged bioproducts. **b**, Lignin primarily comprises three monolignols—*p*-coumaryl and H type lignin units, coniferyl (G type) and sinapyl (S type) alcohols—which are coupled via radical reactions during plant cell wall biosynthesis, generating a complex heterogeneous polymer containing diverse interunit linkages (β-*O*-4, β-β, β-1 and β-5 linkages are shown as examples with G- and S-type units)[1]. Other compounds (hydroxycinnamates, caffeoyl alcohol and flavonoids) can all also be incorporated into or appended to lignin[80]. **c**, Key reactions discussed in this Review within the aromatic catabolic pathways for selected *p*-coumaryl, H-, G- and S-type representative lignin-related compounds (LRCs). Reaction details pertaining to *O*-demethylation (yellow), hydroxylation (green) and decarboxylation (purple) are provided in Figs. 2–4, respectively. Wavy lines indicate known ring-opening positions. FER, ferulate; *p*CA, *p*-coumarate; SAL, syringaldehyde; VAL, vanillin; HBAL, 4-hydroxybenzaldehyde; SA, syringate; VA, vanillate; GUA, guaiacol; 4-HBA, 4-hydroxybenzoate; BEN, benzoate; 3-MGA, 3-*O*-methylgallate; PHE, phenol; BENiol, benzoate-diol; SCY, salicylate; GA, gallate; pyGA, pyrogallol; PCA, protocatechuate; CAT, catechol; GEN, gentisate.

produces a wide variety of methoxylated compounds, including methoxyphenols (for example, guaiacol and syringol), aromatic aldehydes (for example, vanillin and syringaldehyde), aromatic acids (for example, vanillate and syringate) and biaryls (for example, 5,5′-dehydrodivanillate)[7]. Aerobic catabolism of these aromatic compounds makes use of *O*-demethylation to generate diols for ring cleavage. Although there is little difference in the activation of the aromatic ring by a hydroxyl versus a methoxy substituent, deprotonation of the hydroxyls is critical in the proposed mechanisms of both extradiol and intradiol ring-cleaving dioxygenases[23,34]. *O*-demethylation reactions impact a wide variety of biological processes outside aromatic catabolism, including DNA repair, epigenetic modification and gene expression[35,36], and diverse enzymatic mechanisms have evolved to carry out these reactions.

So far, three primary classes of enzymes have been identified that catalyse the *O*-demethylation of LRCs (Fig. 2 and Supplementary Table 1): Rieske oxygenases (ROs)[37,38], cytochromes P450 (P450s)[39] and tetrahydrofolate (THF)-dependent demethylases[40,41]. ROs and

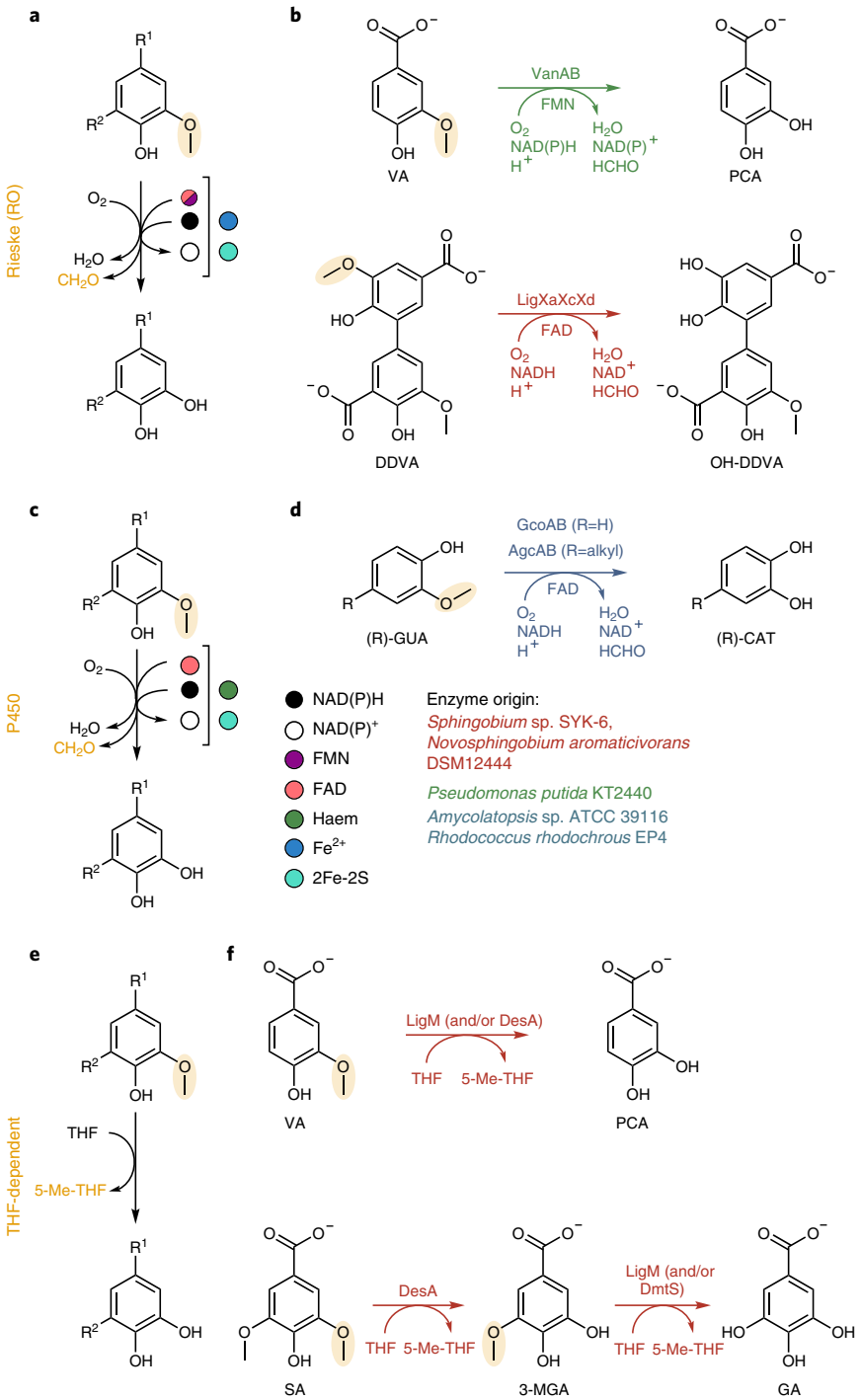

Fig. 2 | Three strategies for aromatic *O*-demethylation. a–**f**, Aerobic bacteria employ the three strategies to carry out lignin-relevant aromatic *O*-demethylation reactions in the context of catabolism: ROs (**a**), including VanAB from KT2440 and the LigXacd enzymes from *Sphingobium* sp. SYK-6 (**b**); P450s (**c**), exemplified by GcoAB from *Amycolatopsis* sp. ATCC 39116 and AgcAB from *Rhodococcus rhodochrous* EP4 (**d**), and THF-dependent mechanisms (**e**), performed by enzymes LigM and DesA from SYK-6 and LigM, DesA and DmtS from *Novosphingobium aromaticivorans* DSM 12444 (**f**). Each strategy is presented in terms of generalized (A, C, E) and specific (B, D, F) reactions, and R groups are used to indicate a range of possible substrates (R^1 = $COOCH_3$, COO^-, CH_2OH, COH or H, and so on; R^2 = OCH_3, OH or H, and so on). VA, vanillate; PCA, protocatechuate; DDVA, 5,5′-dehydrovanillate; OH-DDVA, 2,2′,3-trihydroxy-3′-methoxy-5,5′-dicarboxybiphenyl; GUA, guaiacol; CAT, catechol; SA, syringate; 3-MGA, 3-*O*-methylgallate; GA, gallate.

P450s are typically multi-component systems that utilize a reductase and sometimes a ferredoxin to transfer electrons from NAD(P)H to the oxygenase. The oxygenase components of ROs and P450s contain a mononuclear non-haem iron centre and haem iron, respectively, that catalyse the activation of O_2 and the monooxygenation of the methyl group to produce a hemiacetal intermediate, which breaks down spontaneously to yield the demethylated product along with formaldehyde. For THF-dependent demethylases, the methoxy methyl group is transferred non-oxidatively from the aromatic substrate to the THF cofactor[40,41]. As described in the following, the

catalytic cycles of these enzymes require additional components to regenerate the cofactor. Both ROs and P450s catalyse a wide variety of oxidative chemistries in nature, making them attractive scaffolds for protein engineering and directed evolution to enhance microbial lignin valorization[42,43].

ROs function as two- or three-component systems (Fig. 2a,b and Supplementary Table 1). In two-component systems, a reductase utilizes a flavin coenzyme, either flavin mononucleotide (FMN) or flavin adenine dinucleotide (FAD), to transfer reducing equivalents from NAD(P)H to the oxygenase. Three-component systems have an additional ferredoxin that transfers electrons from the reductase to the oxygenase. The oxygenase itself has a Rieske-type ferredoxin that directs electrons to the mononuclear iron. Substrate binding near the iron ion precedes binding and reductive activation of O_2 at the mononuclear iron. A high-valency ferryl species then hydroxylates the substrate at its reactive *O*-methyl group. Rearrangement of the hydroxylated species gives the ultimate products[34].

ROs involved in the *O*-demethylation of LRCs include VanAB and LigXacd, which catalyse the *O*-demethylation of vanillate and 5,5′-dehydrodivanillate, respectively. VanAB is a Type I-α RO (according to the Kweon classification system[38]) in which VanA is the oxygenase and VanB is an FNR_C-type reductase with a C-terminal [2Fe-2S] domain (F, ferredoxin; N, NAD(P)H; C, C-terminal [2Fe-2S]). LigXacd from *Sphingobium* sp. SYK-6 (SYK-6 hereafter) is a Type III-α RO comprising an oxygenase (LigXa), a ferredoxin (LigXc) and an FNR_N-type FAD/NADH-reductase (LigXd; N, N-terminal [2Fe-2S]). *Pseudomonas putida* KT2440 (KT2440 hereafter), developed as a whole-cell biocatalyst for aromatic catabolism[44], employs VanAB to demethylate vanillate (Fig. 2b)[45,46] and syringate[47]. Either NADH or NADPH may serve as the electron donor, and many orthologues of VanAB can utilize both nicotinamide coenzymes[46,48,49].

P450s constitute a large superfamily of cysteine-ligated haem enzymes[39] that catalyse a variety of stereo- and regioselective reactions, although they are best known for monooxygenation[50]. As in ROs, P450s employ a short electron transport chain to transfer electrons from NAD(P)H to the oxygenase (Fig. 2c,d and Supplementary Table 1). Also as in ROs, bacterial P450s can function as two- or three-component systems with a FAD-containing reductase that reduces the P450 directly or indirectly via a ferredoxin[51]. As a third possible architecture, the P450 and reductase can occur in a single polypeptide[52]. In all cases, substrate binding near the open coordination position over the haem leads to a change in the spin state of the iron, permitting reduction of the metal ion. Binding and reductive activation of O_2 follow, forming a reactive ferryl-haem species. Analogous to the mononuclear non-haem iron RO enzymes, the ferryl species hydroxylates the reactive *O*-methyl group of the substrate, which rearranges to yield formaldehyde and the demethylated product. Electron or hydrogen atom transfer from the reactive C–H bond to the ferryl is often rate-limiting[53].

The first lignin-relevant P450s were identified in *Rhodococcus rhodochrous* and they were observed to demethylate *o*-substituted phenols and *p*-methoxylated benzoates, respectively[54,55]. Other P450s have been shown to demethylate *p*-methoxybenzoate compounds in *Rhodopseudomonas palustris*[56,57]. More recently, GcoAB from *Amycolatopsis* sp. ATCC 39116 was characterized in detail as a tool for *O*-demethylation of the LRC guaiacol to yield catechol (Fig. 2d)[58]. GcoA belongs to the CYP255A family. GcoB, the cognate reductase, is analogous to the FNR_N-type reductase component of ROs[38], with a FAD-containing domain and an N-terminal [2Fe-2S] ferredoxin domain. Somewhat unusually, GcoAB forms a stable complex[58,59]. GcoAB catalyses the *O*-demethylation of a variety of aromatic substrates in addition to guaiacol[59,60]. This promiscuity, combined with comprehensive structural studies of the GcoA active site, enabled the substitution of active-site residues to expand the substrate range to include syringol[60], *o*-vanillin and *p*-vanillin[61]. Finally, AgcAB, which is found in two *Rhodococcus* species and shares over 50% amino-acid sequence identity with GcoAB, catalyses the *O*-demethylation of larger, 4-alkylguaiacol substrates to yield 4-alkylcatechols (Fig. 2d)[62].

Recent interest in lignin-relevant P450s from bacteria[63] demonstrates continued opportunity for enzyme discovery. For example, preliminary studies identified guaiacol-specific *O*-demethylases in *Corynebacterium*[64], *Streptomyces*[65] and *Moraxella*[66], but no further metabolic or protein engineering has been reported. Heterologous expression of a two-component P450 *O*-demethylase system from *R. rhodochrous* J3 enabled *P. putida* EM42 to grow on guaiacol[67], and a new CYP199A25 from *Arthrobacter* was identified as a *p*-methoxybenzoate demethylase[68]. Furthermore, the P450BM3 fusion protein has been employed in a synthetic peroxygenase system to regio-selectively *O*-demethylate several aromatic ethers[69]. Interestingly, to our knowledge, no P450 *O*-demethylases have yet been reported for the utilization of vanillate or syringate.

Aerobic bacteria employ a third, non-oxidative mechanism for aromatic *O*-demethylation, in which THF serves as the acceptor of the methyl group (Fig. 2e,f and Supplementary Table 1). Unlike ROs and P450s, THF-dependent *O*-demethylases do not generate formaldehyde as a by-product, thereby avoiding the cytotoxicity and enzyme inhibition associated with this compound[48,49,70]. In SYK-6, two enzymes catalyse THF-dependent *O*-demethylation reactions: LigM demethylates vanillate and 3-*O*-methylgallate, and DesA preferentially demethylates syringate (Fig. 2f)[40,41]. In these reactions, transfer of the methyl group produces 5-methyl-THF, an essential intermediate in C1 metabolism for the biosynthesis of methionine[71,72]. THF is regenerated by MetF and LigH[15,41]. Crystal structures of LigM reveal that the enzyme forms a cloverleaf shape with a large central cavity to accommodate THF and the substrate[73,74]. A tyrosine serves as an acid to the substrate methoxy oxygen, facilitating methyl transfer to THF-N_5. Recently, LigM and DesA homologues were characterized in *Novosphingobium aromaticivorans* DSM 12444, along with a new *O*-demethylase, DmtS, which converts 3-*O*-methylgallate to gallate (Fig. 2f)[75]. LigM and DesA homologues are also present in *Agrobacterium tumefaciens* C58 and *Rubrobacter xylanophilus* DSM 9941[41], and have been identified in thermophilic lignin-degrading microbial communities analysed using stable isotope probing (Levy-Booth, D. J. et al.; manuscript in preparation). This latter study highlights the considerable potential of metagenomic approaches for identifying enzymes for lignin bioconversion. Furthermore, several methyltransferase systems catalyse *O*-demethylation in anaerobic bacteria[76–79], but their activity may be oxygen-labile, potentially limiting their use in aerobic industrial bioprocessing.

Aromatic hydroxylation

Hydroxylation of the aromatic ring is a key strategy for generating activated aromatic diols. LRCs for aromatic hydroxylation include monomers derived from *p*-hydroxyphenyl-type lignin as well as aromatic acids that are frequently esterified to lignin or hemicellulose, such as 4-hydroxybenzoate (4-HBA), *p*-coumarate and hydroxyphenylacetate[80]. Flavin monooxygenases (FMOs)[81] comprise the main class of enzymes that catalyse mono-hydroxylation of LRCs (Fig. 3 and Supplementary Table 2). Three other classes of aromatic hydroxylase have been reported: ROs[82], P450s and pterin-dependent enzymes[83]. However, only hydroxylation by P450s has been identified in natural lignin-relevant catabolic reaction pathways thus far, and only in fungal hosts, to our knowledge[84,85]. In plants, three P450s—CYP73A, CYP98A and CYP84—catalyse three phenyl ring hydroxylation steps in monolignol biosynthesis, which modulates the H/G/S ratio of the monolignol pool[86]. Other aromatic and xenobiotic compounds that are not typically considered LRCs, often containing hydroxyl substituents at the *m*- or *o*-position (such as 3-hydroxybenzoate and salicylate, respectively), as well

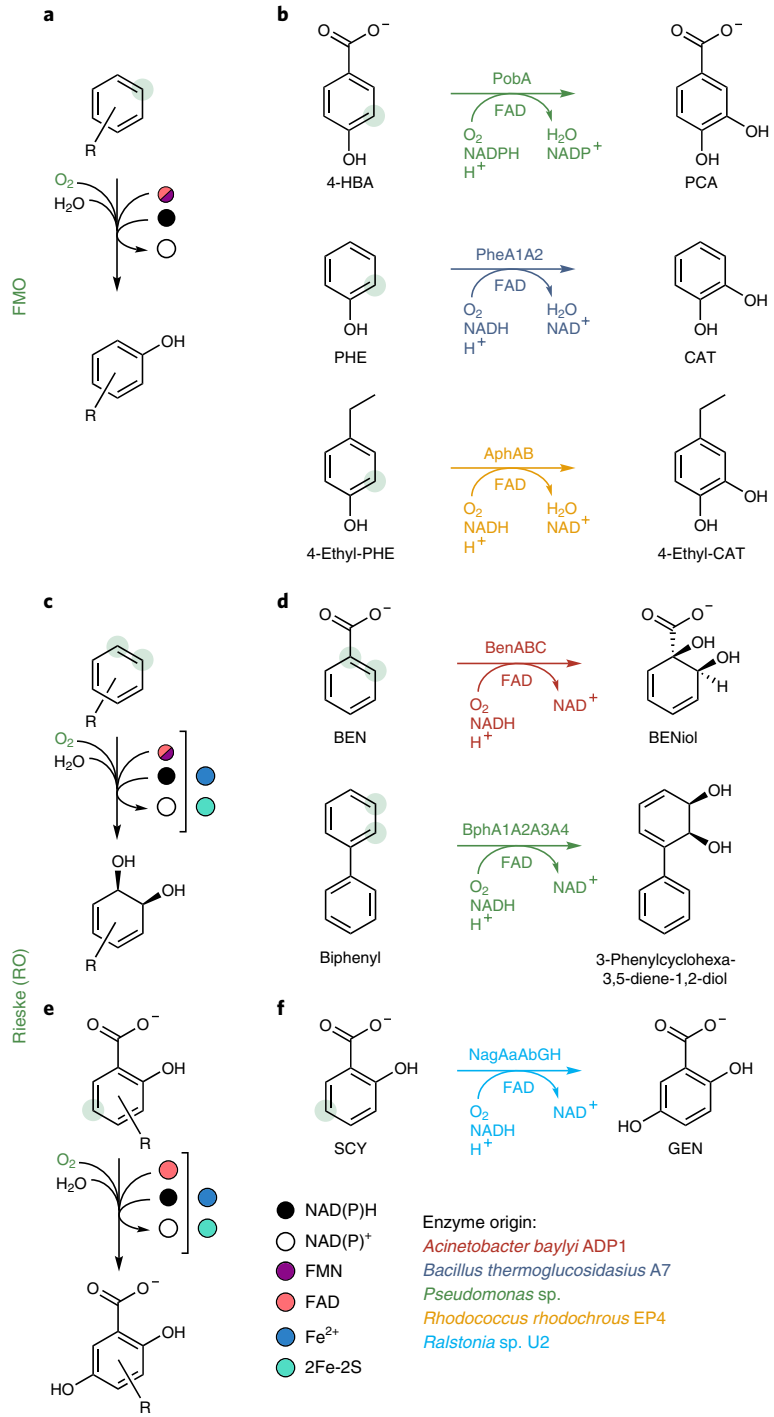

Fig. 3 | Strategies for aromatic hydroxylation. a,**b**, Examples are provided from five bacteria including the FMO-dependent mechanism (**a**) performed by the single-component FMO PobA from *Pseudomonas fluorescens*, as well as the two-component FMOs PheA1A2 from *Bacillus thermoglucosidasius* A7 and AphAB from *Rhodococcus rhodochrous* EP4 (**b**). **c**–**f**, A second strategy utilizes ROs that perform either dihydroxylation (**c**) or or monooxygenation (**e**) of the aromatic ring. f, Generalized (**a**,**c**,**e**) and specific (**b**,**d**,**f**) reactions are shown, and R groups are used to indicate a range of possible substrates (R = CH_2COO^-, CH_2CH_3, COO^-, OH or H, and so on). 4-HBA, 4-hydroxybenzoate; PCA, protocatechuate; PHE, phenol; CAT, catechol; BEN, benzoate; BENiol, benzoate-diol; SCY, salicylate; GEN, gentisate.

as phenol and benzoate are also subject to ring hydroxylation in preparation for ring cleavage. Among the ring-hydroxylating ROs, those that transform the non-LRC compounds phenol[87], naphthalene[88], salicylate[89], biphenyl[90] and benzoate[91] have been well studied and could serve as scaffolds for protein and metabolic engineering efforts. Although these compounds are not common LRCs, these scaffolds could prove useful in overcoming bottlenecks in aromatic catabolic pathways.

FMOs employ a flavin cofactor to activate O_2 (vide infra), forming a C4a-hydroperoxyflavin intermediate, which subsequently introduces one oxygen atom into the substrate (Fig. 3a,b and Supplementary Table 2). Two types of FMO catalyse lignin-relevant

aromatic hydroxylation reactions: one-component systems that bind FAD as a prosthetic group, and two-component systems that utilize FAD, FMN or riboflavin[81].

Single-component FMOs contain a Rossmann fold to ensure tight association of FAD with the active site throughout the catalytic cycle[81]. Both flavin reduction and substrate oxidation occur within the active site. Single-component FMOs use NAD(P)H to directly reduce the flavin, where hydride transfer from the NAD(P)H to flavin takes place rapidly given the transient coordination of the nicotinamide. These enzymes demonstrate regioselective hydroxylation, high substrate specificity, as well as strong control over the bound flavin, potentially as a mechanism to avoid futile consumption of the nicotinamide cofactor. The single-component FMO 4-hydroxybenzoate-3-monooxygenase, also known as PHBH, from *Pseudomonas fluorescens* and other pseudomonads has been the subject of several decades of biochemical and structural studies[92]. Orthologues of PHBH are found widely among aromatic catabolic bacteria, but these orthologues demonstrate diversity in their preference and specificity for NADH or NADPH[93–95].

Two-component FMOs diverge structurally and mechanistically from single-component systems[96]. As their name implies, these enzymes utilize two proteins to carry out monooxygenation of the aromatic substrate: a reductase component that reduces the flavin using NAD(P)H, and an oxygenase component that accepts the reduced flavin and catalyses hydroxylation of the substrate. Whereas the flavin moiety in single-component FMOs can rapidly transition between conformations in the oxidized state[92], thereby facilitating a transient interaction with the nicotinamide cofactor, two-component FMOs only accept a reduced flavin from a reductase partner[97]. For two-component FMOs, although the reductase can reduce the flavin in the absence of substrate[98], the presence of substrate stimulates flavin reduction in some reductases[99]. Binding of the correct substrate triggers flavin motion towards the bound NAD(P)H in FMOs, initiating the catalytic cycle[100].

A number of two-component FMOs that transform LRCs have been characterized. PheA1A2 from *Bacillus thermoglucosidasius* A7 hydroxylates phenol to generate catechol (Fig. 3b)[101], which is subject to *ortho*-cleavage in this strain. AphAB from *Rhodococcus rhodochrous* EP4 catalyses the hydroxylation of the 4-alkylphenols to 4-alkylcatechols (Fig. 3b), which are subject to *meta*-cleavage by the enzyme AphC[102]. Structures for these two-component FMOs have yet to be reported. The best characterized two-component FMO is 4-hydroxyphenylacetate hydroxylase (HPAH), which catalyses the hydroxylation of 4-hydroxyphenylacetate (HPA)[99,103] to 3,4-dihydroxyphenylacetate (DHPA) (Supplementary Table 2). 4-Hydroxyphenylacetate (HPA) is a minor component of softwood lignin streams, but structural and mechanistic insights gleaned from 4-hydroxyphenylacetate hydroxylase (HPAH) provide a foundation for understanding the activity of two-component FMOs on diverse substrates.

In the context of lignin catabolism, ROs are important for *O*-demethylation (vide supra) and for performing ring hydroxylation in the lower pathways. ROs are also instrumental in the catabolism of many xenobiotics and compounds that are not lignin-relevant. Therefore, hydroxylation reactions mediated by ROs are described here for comparison to the FMO reaction paradigm (Fig. 3c–f). For example, the biphenyl (5-5) linkage between aromatic groups is commonly found in lignin[104], and degradation pathways for biphenyl compounds have been identified in multiple species of soil bacteria[90]. In pseudomonads and rhodococci, biphenyl dioxygenase is a three-component system composed of four proteins: BphA1 and BphA2, which together form the oxygenase component, BphA3 (the ferredoxin) and BphA4 (the ferredoxin reductase) (Fig. 3d)[90]. In these systems, the large subunit of the oxygenase harbours the active site[105], making it an ideal target for engineering substrate recognition and specificity. Although many ROs catalyse dihydroxylation reactions, others catalyse the monooxygenation of hydroxylated aromatic compounds (Fig. 3e)[106]. One example is salicylate 5-hydroxylase (S5H) from *Ralstonia* sp. U2, which catalyses hydroxylation of salicylate to form gentisate (Fig. 3f). Salicylate 5-hydroxylase (S5H) is composed of NagAaAbGH and displays similar specificity for NADH and NADPH[107]. Mirroring the example of GcoAB presented above, mutation of RO active-site residues has led to expansion of the repertoire of chemistries performed and substrates accepted by these enzymes[108–110].

Decarboxylation

Analogous to *O*-demethylation and hydroxylation, aromatic decarboxylation can prime LRCs for ring-opening. Aromatic decarboxylation can be classified into two mechanistic types: reductive and oxidative. These are distinguished by the substitution of the carboxylate by either a hydride or a hydroxyl group, respectively (Fig. 4 and Supplementary Table 3). Reductive aromatic decarboxylases typically belong to the amidohydrolase superfamily (AHS) or the prenylated FMN (PrFMN) utilizing UbiD-related protein family. Two enzyme classes are known to perform oxidative decarboxylation: ROs and FMOs. These processes, exemplified by salicylate 1-hydroxylase (PhnIIA3A4)[111], appear to be limited to *o*- and *p*-hydroxylated forms of hydroxybenzoates, perhaps because this configuration facilitates charge delocalization between the hydroxyl and carboxylate during the catalytic cycle. The relative positioning of carboxylates and hydroxyl groups on the ring dictates which enzyme type(s) may be utilized for decarboxylation. In the aerobic bacterial catabolism of LRCs, the decarboxylation reactions described so far proceed predominantly through the reductive route. Oxidative decarboxylation of LRCs is found in fungal systems[112], and oxidative aromatic decarboxylation is prevalent in the bacterial catabolism of non-LRC aromatics, originating from hydrocarbons, including phthalate isomers. Examples of well-studied oxidative decarboxylation pathways are included for comparison with the reductive decarboxylation reaction paradigm.

Decarboxylation of *o*-substituted compounds may proceed by a reductive decarboxylation mechanism, mediated by AHS enzymes. Members of this superfamily typically catalyse the hydrolysis of an ester or amide bond at a carbonyl or phosphoryl centre[113,114]. However, a subfamily of AHS enzymes (COG2159) catalyse decarboxylation (Fig. 4a)[115–117]. This subfamily has the distorted triose-phosphate isomerase (TIM)-barrel structure characteristic of the superfamily and a metal ion in the active site. The AHS-type decarboxylases are exemplified by LigW from SYK-6, which catalyses the decarboxylation of 5-carboxyvanillate to vanillate and CO_2. LigW contains a catalytically essential Mn^{2+}, although other decarboxylases contain Zn^{2+}. In AHS-type hydrolases, the metal ion coordinates water, activating it for nucleophilic attack. By contrast, in the carboxylases, the metal ion binds the substrate in a bidentate manner via the hydroxyl and carboxyl groups, promoting distortion of the aromatic ring and charge delocalization to facilitate C–C bond fission[113,116]. The reaction proceeds by protonation of the carbon adjacent to the carboxylate group, which departs as CO_2 (refs. [116,118]). Interestingly, SYK-6 harbours a second copy of 5-carboxyvanillate decarboxylase, LigW2, but the function of this redundancy remains poorly understood[119]. Other examples of AHS-type decarboxylases include ro01859 from *Rhodococcus jostii* RHA1 and ag00121 from an *Agrobacterium* species. These enzymes were recently proposed to be involved in the production of 1,2,4-benzenetriol, or hydroxyquinol, as part of an alternative pathway for beta-ketoadipate production from protocatechuate, gentisate (2,5-dihyroxybenzoate) and 2,6-dihydroxybenzoate[120,121]. Reductive decarboxylation may also be catalysed by an NTF2-type enzyme scaffold, as exemplified by a gallate/protocatechuate decarboxylase described in several fungal species, for which a bacterial equivalent has not been identified[122–124].

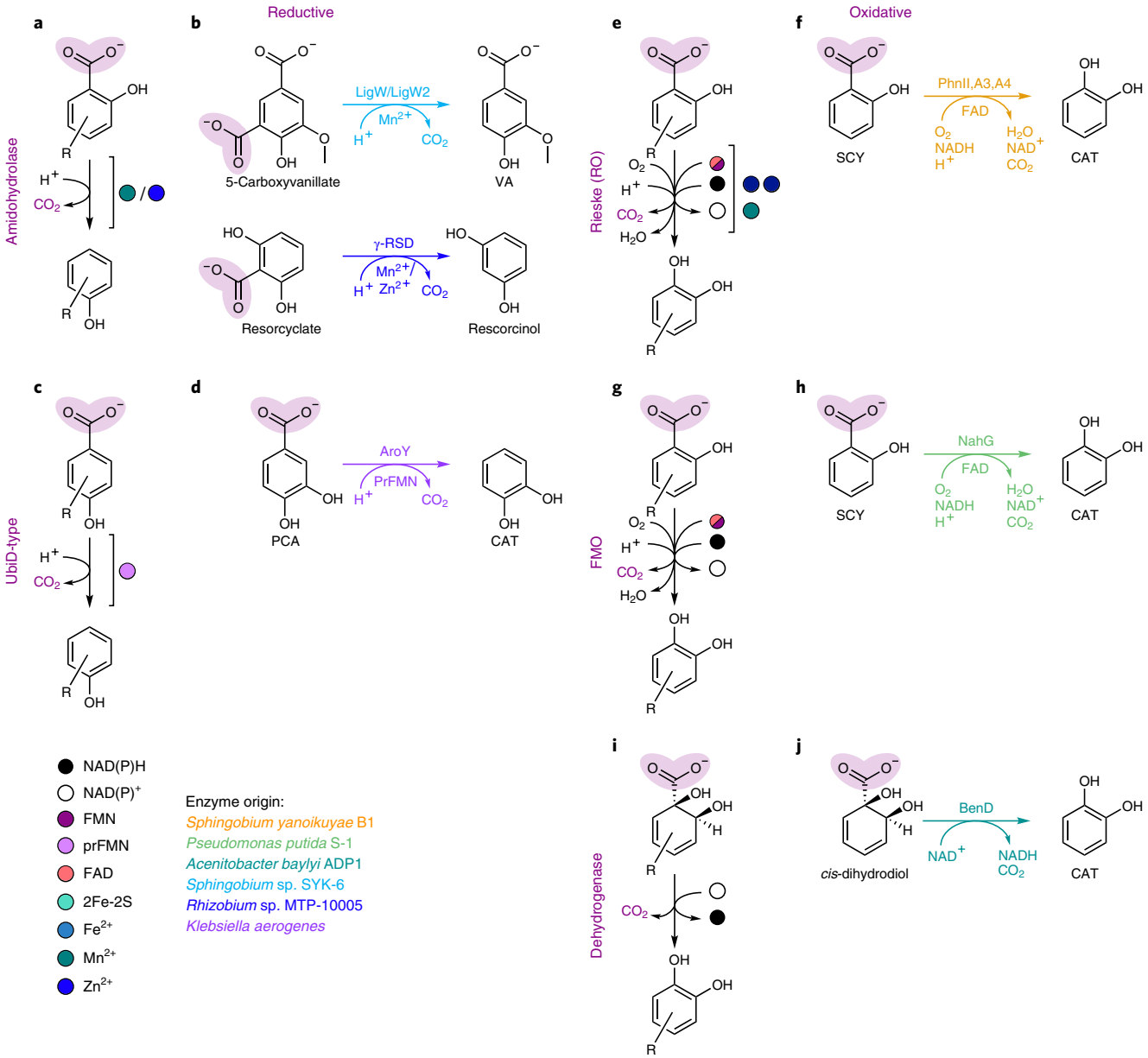

Fig. 4 | Reductive and oxidative strategies for aromatic decarboxylation. a–d, Two reductive decarboxylation strategies: AHS systems (**a**), including LigW/LigW2 and γ-RSD (**b**), and the UbiD-type system (**c**), including representative enzyme AroY (**d**). **e–j**, Three oxidative strategies: ROs (**e**), including PhnIIPhnA3A4 (**f**), FMOs (**g**), including the single-component NahG (**h**), and *cis*-dihydrodiol dehydrogenases (**i**), including BenD (**j**). Generalized (**a**,**c**,**e**,**g**,**i**) and specific (**b**,**d**,**f**,**h**,**j**) reactions are shown, where R groups are used in the generalized schemes to indicate a range of possible substrates. VA, vanillate; PCA, protocatechuate; CAT, catechol; SCY, salicylate.

A second class of enzymes that catalyse the reductive decarboxylation of LRCs is the UbiD-family enzymes (Fig. 4c). These enzymes require a unique PrFMN cofactor, which is produced by UbiX, a prenyl transferase (Fig. 5)[125]. Genes encoding this system typically occur in a BCD cluster where enzyme B encodes the prenyl transferase, C encodes the UbiD-type decarboxylase, and D is an open reading frame of unknown function[126,127]. Interestingly, the D element is not commonly found in clusters encoding the prototypical UbiX/UbiD ubiquinone pair[126]. To form the PrFMN cofactor, UbiX first catalyses the formation of a fourth, non-aromatic ring in the FMN isoalloxazine moiety using dimethylallyl phosphate or dimethylallyl pyrophosphate as a prenyl donor[125,128]. The newly synthesized cofactor is then transferred to the decarboxylase and undergoes an oxidative maturation step to the active $PrFMN_{iminium}$ form[128,129]. The decarboxylase itself, UbiD, requires potassium and divalent metal ions, such as manganese or iron, to properly bind the flavin cofactor[128]. Importantly, FMN prenylation prevents the two-electron redox chemistry that commonly occurs in flavoenzymes[130]. Two reaction mechanisms have been proposed for this class of enzyme, involving 1,3-cyclodipolar addition and a quinoid intermediate for polarophile and non-polarophile substrates, respectively[128,131]. Notable examples of a UbiD-type decarboxylase include AroY enzymes from *Klebsiella* sp. and *Enterobacter* sp., which catalyse the conversion of protocatechuate to catechol (Fig. 4d)[132,133].

Aromatic oxidative decarboxylation performed by FMOs and ROs is described for many xenobiotic and non-LRCs. Examples of oxidative LRC decarboxylation are sparse, but have been observed in fungi, including transformation of 4-HBA and gallate to hydroquinone

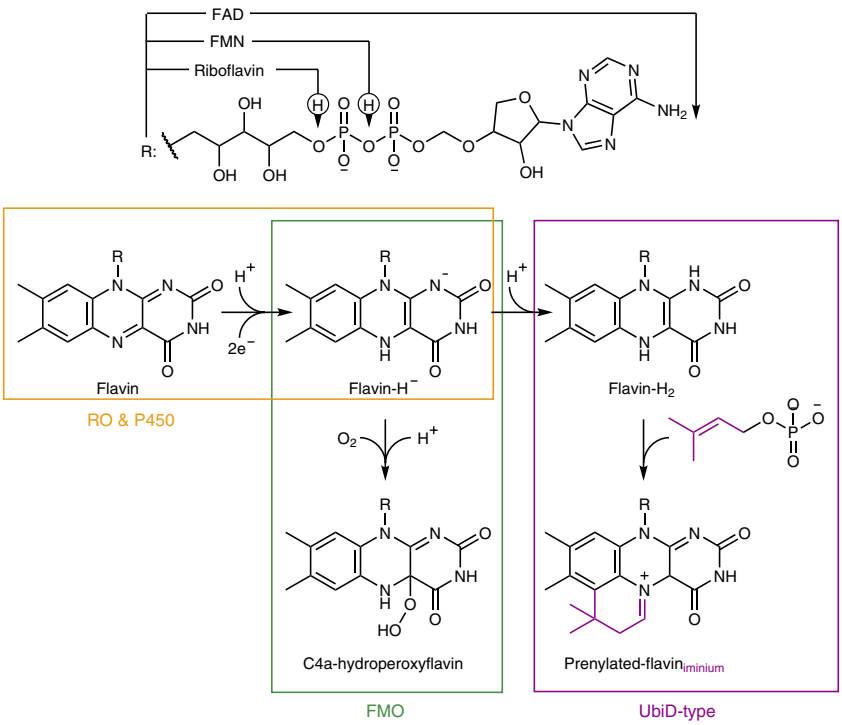

Fig. 5 | Forms and functions of flavin cofactors in the catabolism of LRCs. Flavin cofactors are derived from a riboflavin (vitamin B_2), which comprises an isoalloxazine group with a ribityl group attached to the central ring. The ribityl group of riboflavin can be further functionalized with a phosphate or an adenine diphosphate to form FMN and FAD, respectively. The alloxazine ring may also be modified to form a prenylated FMN (PrFMN). Without prenylation, flavins are used to shuttle two electrons from NAD(P)H towards a substrate[130]. This two-electron shuttle function is found in the reductase component of ROs and P450s. Alternatively, fully reduced flavin can react with O_2 to form a flavo-hydroxyperoxide adduct, which is utilized as the hydroxylating moiety by FMO-type hydroxylases[165,166]. This redox cycling capacity, however, is lost upon prenylation; instead, the modified flavin cofactor gains a new functionality in catalysing decarboxylation in the UbiD-type system[167].

and pyrogallol, respectively[134]. FMOs, ROs, as well as the accompanying dehydrogenases, offer attractive scaffolds for engineering towards an expanded slate of aromatic substrates accessible to an organism, or towards overcoming bottlenecks in aromatic catabolic pathways. For example, PhnIIA3A4 and NahG, two salicylate 1-hydroxylases, which are a RO and FMO, respectively (Fig. 4e–h), display reaction mechanisms mirroring processes described in the previous sections[135–137]. Although uncommon, *o*-hydroxybenzoate LRCs may arise from partial processing of aromatic dimers, such as in the case of 5-carboxyvanillate for 5,5′-dehydrodivanillate. Some RO-mediated reactions, however, produce *cis*-dihydrodiols, which necessitate subsequent dehydrogenation to generate the corresponding catechol (Fig. 4i)[138]. For example, in the catabolism of benzoate, another non-LRC, the BenABC enzyme system catalyses the dihydroxylation of benzoate to (*Z*)-1,6-dihydroxycyclohexa-2,4-diene-1-carboxylate (Fig. 3d), which is in turn oxidized by the dehydrogenase BenD to form catechol using NAD(P)$^+$ as the electron acceptor (Fig. 4j)[91,111,139]. The parallel decarboxylation strategies employed for the catabolism of LRCs and xenobiotics highlight the intersections of these pathways, and suggest these reaction paradigms could be adapted for lignin valorization as well as bioremediation.

Translating biochemical insights for improved in vivo function

O-demethylation, hydroxylation and decarboxylation are often rate-limiting steps in microorganisms engineered to convert LRC mixtures to single products[13,27,29,31–33]. Despite robust characterization in vitro, the relative advantages and disadvantages of each biochemical paradigm when implemented in vivo remain largely unknown. Chassis selection and optimization, a critical component to achieve success in vivo, has been reviewed elsewhere[19,140]. Here we highlight selected challenges and opportunities for translating biochemical insights to tailored microbes for lignin valorization.

Many of the enzymes discussed here rely on reducing equivalents, suggesting that equipping strains for LRC conversion with systems for maintaining redox balance will be critical for successful application. For example, it was recently shown that the PHBH analogue PobA[137] introduces a bottleneck leading to 4-HBA accumulation in KT2440 due to an unfavourable NADP$^+$/NADPH ratio[141]. By replacing PobA, which accepts only NADPH, with an exogenous enzyme, PraI, which accepts both NADH and NADPH[141], the 4-HBA bottleneck was overcome. In another approach, the addition of formate to KT2440 fermentations activated endogenous NAD$^+$-dependent formate dehydrogenases, thereby increasing the rate of NADH regeneration[142]. Diverse fungal hydroxylases[112,134,143] also present an intriguing source for improved hydroxylation. As more enzymes catalysing redox chemistries are engineered into a single microbial chassis, cofactor engineering will be essential to maintain cell viability and efficient biocatalytic function[51,144].

Similarly, metabolic engineering strategies should consider the production of required coenzyme(s) in tandem with expression of the cognate enzyme. For example, a bottleneck in protocatechuate decarboxylation to form catechol by the UbiD-like decarboxylase AroY has been reported[31,32]. Recent efforts improved strain performance by increasing the availability of PrFMN, the coenzyme for AroY, via overexpression of an additional prenyl transferase[30] or enzymes involved in the production of the precursor dimethylallyl phosphate[129]. This example indicates the importance of engineering

robust production of coenzyme, especially when the exogenous enzyme system requires non-native or low-abundance coenzymes.

In the case of multi-component enzyme systems, balanced expression of each component is often required to optimize activity in engineered hosts. For example, adequate turnover of 4-methoxybenzoate by the *R. palustris* CYP199A4 demethylase system in *Escherichia coli* required additional ferredoxin, HaPux, which was achieved by expressing two copies of the associated gene[145]. Similarly, modulating the ratio of partner redox proteins in a myxobacterial CYP260A1 system affected the P450 catalytic activity as well as product profiles[146]. In cases where analogous single- and multi-component systems are available, the metabolic burden of expressing a larger enzyme versus two smaller enzymes should be considered. Finally, enzyme stability is another critical yet largely unexplored area. Evaluating protein stability, and engineering chaperones or co-translational folding when necessary[147], is a burgeoning area of research.

The potential flexibility of partner interactions in multi-component systems presents an interesting opportunity to engineer increased turnover and expanded substrate specificity. Electron transfer between the substrate and haem-ferryl in P450s[53], or the reductase in ROs[148], can be rate-limiting. Detailed characterization of cofactors, including redox potentials, electron transport pathways, component complexes and the active-site features that facilitate efficient electron delivery and catalysis, offer multiple routes to engineer faster turnover and thereby improve flux. With regard to substrate specificity, recent studies highlight that flexible redox partner combinations for bacterial P450s may have important implications for function and specificity[149]. The use of electron transport chains as scaffolds for engineering new substrate specificities to access additional LRCs, or redirect flux in a desirable way, is a compelling opportunity for future work.

The cytotoxicity of substrates, intermediates and by-products should be considered and mitigated where possible. Indeed, accumulation of cytotoxic intermediates or by-products may be a differentiating feature towards achieving in vivo success. For example, RO- and P450-mediated *O*-demethylation generates formaldehyde, whereas THF-dependent systems generate 5-methyl-THF. Formaldehyde is an acutely toxic compound for which microorganisms have a variety of detoxification pathways[150]. Thus, it is plausible that engineering-enhanced formaldehyde detoxification will improve the utility of RO- or P450-based biocatalysts, especially in heterologous hosts. Indeed, the coupled action of formaldehyde dehydrogenase and formate dehydrogenase can regenerate two units of NADH for the cell, and formaldehyde utilization via the ribulose monophosphate (RuMP) cycle has been shown to mitigate toxicity and avoid waste of carbon in KT2440[151]. In vivo, tolerance adaptive laboratory evolution could be useful in mitigating formaldehyde toxicity by leveraging natural selection to identify non-intuitive genetic targets for improving growth[152,153]. Alternatively, spatial partitioning of reactions that generate toxic by-products to outer membrane vesicles, which natively contribute to aromatic catabolism in KT2440[154] and can be engineered to carry active enzymes[155], holds promise to decrease intracellular toxicity. Finally, utilization of dynamic metabolic control to mitigate toxicity is another compelling and proven strategy for metabolic engineering[156].

Given the systems-level complexity that ultimately governs the efficiency and success of microbial cell factories, direct comparisons between multiple paradigms may guide selection for a given application. For example, vanillate *O*-demethylation by the RO VanAB represents a rate-limiting step in the production of muconate from LRCs[33]. Bacteria typically employ just one of the three enzymatic strategies for *O*-demethylation of a given substrate, but replacing or supplementing VanAB with a P450 system or a THF-dependent *O*-demethylase and directly comparing muconate production could reveal whether a heterologous system outperforms the native VanAB. Further investigation to uncover the underlying reason for improved strain performance could provide insight into why a particular biocatalytic mechanism is optimal for a given system in a holistic context, in comparison to evaluating the in vitro performance of an enzyme for a given substrate in isolation. Furthermore, these comparisons can provide targets for continued in vivo optimization.

The evaluation of combinatorial enzyme:chassis systems will require the development of robust in vivo screening methods. A fluorescent biosensor paired with fluorescence activated cell sorting[157] or high-throughput selection assays coupled to growth[158] are options that have been successfully implemented in microbial chassis for the optimization of LRC catabolism[159]. However, the utilization of transcription factor-based biosensors requires genetic tractability and is often host-specific, limiting applicability by chassis. Metabolic flux analysis for the quantification of intracellular fluxes within a network[160], both at the node of interest as well as central carbon metabolic pathways, can provide insight into the broader cellular demands of one strategy versus another.

As bottlenecks in metabolite turnover are overcome, efficient uptake of LRCs may become limiting. Aromatic carboxylates are not predicted to passively permeate the bacterial membrane[161], suggesting the requirement for a transporter system for many of the LRCs discussed here. Identification and characterization of import mechanisms for LRCs of interest in model chassis, as was recently done in KT2440[162], is an important first step towards engineering uptake systems for high productivities. Colocalization of enzymes within a pathway by engineered protein scaffolds and metabolons is an established strategy for increasing flux through diverse pathways[163,164] that could be targeted to membranes for localized activity upon substrate import.

Summary and outlook

Aromatic *O*-demethylation, hydroxylation and decarboxylation are catalysed by multiple enzymatic paradigms that differ in cofactor utilization and enzyme class. Often, the critical enzymes performing these reactions vary in rate, stability and in vivo activity, all details that factor into their use in biotechnological applications. Comparisons of similar chemistries mediated by different enzyme classes will ultimately inform rational metabolic engineering, synthetic biology and cell-free conversion technologies. When bringing together pathway components from diverse microbes into engineered systems, optimization becomes a non-trivial, multi-variable problem. Among these variables, cofactor and coenzyme availability and utilization can play a large role in mediating flux through the pathway, but other factors intrinsic to the native system may also play a critical role in successful biocatalysis, and these factors may be harder to predict and control. Although many enzymes that conduct important biochemical reactions in aromatic catabolic pathways have been extensively characterized, exciting opportunities in biological lignin valorization should encourage renewed focus on these pathways and their potential application in industrial bioprocessing.

Received: 1 June 2021; Accepted: 18 January 2022;
Published online: 25 February 2022

References

1. Boerjan, W., Ralph, J. & Baucher, M. Lignin biosynthesis. *Annu. Rev. Plant Biol.* **54**, 519–546 (2003).
2. del Río, J. C. et al. Lignin monomers from beyond the canonical monolignol biosynthetic pathway: another brick in the wall. *ACS Sustain. Chem. Eng.* **8**, 4997–5012 (2020).
A review of recent findings that valuable aromatic compounds, such as flavonoids, hydroxystilbenes, and hydroxycinnamic amides, can act as genuine lignin monomers in some plant species, challenging the conventional view of lignin composition and assembly.

3. Ralph, J. Hydroxycinnamates in lignification. *Phytochem. Rev* **9**, 65–83 (2010).
4. Davis, R. et al. *Process Design and Economics for the Conversion of Lignocellulosic Biomass to Hydrocarbons*: *Dilute-Acid Prehydrolysis and Enzymatic Hydrolysis Deconstruction of Biomass to Sugars and Biological Conversion of Sugars to Hydrocarbons* (NREL, 2013).
5. Corona, A. et al. Life cycle assessment of adipic acid production from lignin. *Green Chem.* **20**, 3857–3866 (2018).
6. Zakzeski, J., Bruijnincx, P. C. A., Jongerius, A. L. & Weckhuysen, B. M. The catalytic valorization of lignin for the production of renewable chemicals. *Chem. Rev.* **110**, 3552–3599 (2010).
7. Ragauskas, A. J. et al. Lignin valorization: improving lignin processing in the biorefinery. *Science* **344**, 1246843 (2014).
8. Rinaldi, R. et al. Paving the way for lignin valorisation: recent advances in bioengineering, biorefining and catalysis. *Angew. Chem.* **55**, 8164–8215 (2016).
9. Schutyser, W. et al. Chemicals from lignin: an interplay of lignocellulose fractionation, depolymerisation and upgrading. *Chem. Soc. Rev.* **47**, 852–908 (2018).
10. Sun, Z., Fridrich, B. L., de Santi, A., Elangovan, S. & Barta, K. Bright side of lignin depolymerization: toward new platform chemicals. *Chem. Rev.* **118**, 614–678 (2018).
11. Linger, J. G. et al. Lignin valorization through integrated biological funneling and chemical catalysis. *Proc. Natl Acad. Sci. USA* **111**, 12013–12018 (2014).
12. Bugg, T. D. H. & Rahmanpour, R. Enzymatic conversion of lignin into renewable chemicals. *Curr. Opin. Chem. Biol.* **29**, 10–17 (2015).
13. Beckham, G. T., Johnson, C. W., Karp, E. M., Salvachúa, D. & Vardon, D. R. Opportunities and challenges in biological lignin valorization. *Curr. Opin. Biotechnol.* **42**, 40–53 (2016).
14. Abdelaziz, O. Y. et al. Biological valorization of low molecular weight lignin. *Biotechnol. Adv.* **34**, 1318–1346 (2016).
15. Kamimura, N. et al. Bacterial catabolism of lignin-derived aromatics: new findings in a recent decade: update on bacterial lignin catabolism. *Environ. Microbiol. Rep.* **9**, 679–705 (2017).
16. Eltis, L. D. & Singh, R. in *Lignin Valorization*: *Emerging Approaches* Vol. 19 (ed. Beckham, G. T.) 290–313 (The Royal Society of Chemistry, 2018).
17. Seaton, S. C. & Neidle, E. L. in *Lignin Valorization*: *Emerging Approaches* Vol. 19 (ed. Beckham, G. T.) 252–289 (The Royal Society of Chemistry, 2018).
18. Liu, Z.-H. et al. Identifying and creating pathways to improve biological lignin valorization. *Renew. Sust. Energ. Rev.* **105**, 349–362 (2019).
19. Becker, J. & Wittmann, C. A field of dreams: lignin valorization into chemicals, materials, fuels and health-care products. *Biotechnol. Adv.* **37**, 107360 (2019).
A comprehensive review of technological advances in lignin recovery, breakdown, and conversion, particularly by microbial cell factories, that are enabling the first sustainable value chains using lignin.
20. Vardon, D. R. et al. Adipic acid production from lignin. *Energy Environ. Sci.* **8**, 617–628 (2015).
21. Fuchs, G., Boll, M. & Heider, J. Microbial degradation of aromatic compounds—from one strategy to four. *Nat. Rev. Microbiol.* **9**, 803–816 (2011).
22. Bugg, T. D. Dioxygenase enzymes: catalytic mechanisms and chemical models. *Tetrahedron* **59**, 7075–7101 (2003).
23. Vaillancourt, F. H., Bolin, J. T. & Eltis, L. D. The ins and outs of ring-cleaving dioxygenases. *Crit. Rev. Biochem. Mol.* **41**, 241–267 (2006).
24. Mycroft, Z., Gomis, M., Mines, P., Law, P. & Bugg, T. D. H. Biocatalytic conversion of lignin to aromatic dicarboxylic acids in *Rhodococcus jostii* RHA1 by re-routing aromatic degradation pathways. *Green Chem.* **17**, 4974–4979 (2015).
25. Becker, J., Kuhl, M., Kohlstedt, M., Starck, S. & Wittmann, C. Metabolic engineering of *Corynebacterium glutamicum* for the production of *cis*, *cis*-muconic acid from lignin. *Micro. Cell Fact.* **17**, 115 (2018).
26. Higuchi, Y. et al. Discovery of novel enzyme genes involved in the conversion of an arylglycerol-β-aryl ether metabolite and their use in generating a metabolic pathway for lignin valorization. *Metab. Eng.* **55**, 258–267 (2019).
27. Johnson, C. W. et al. Innovative chemicals and materials from bacterial aromatic catabolic pathways. *Joule* **3**, 1523–1537 (2019).
The production of 16 metabolites of bacterial aromatic catabolism and their use in producing materials with superior properties relative to petroleum-derived analogs.
28. Li, X. et al. Discovery of potential pathways for biological conversion of poplar wood into lipids by co-fermentation of *Rhodococci* strains. *Biotechnol. Biofuels* **12**, 60 (2019).
29. Perez, J. M. et al. Funneling aromatic products of chemically depolymerized lignin into 2-pyrone-4-6-dicarboxylic acid with *Novosphingobium aromaticivorans*. *Green Chem.* **21**, 1340–1350 (2019).
S-, G- and H-type lignin monomers are biologically funnelled to a single product, 2-pyrone-4,6-dicarboxyic acid, in *Novosphingobium aromaticivorans* DSM 12444.
30. Suzuki, Y. et al. Development of the production of 2-pyrone-4,6-dicarboxylic acid from lignin extracts, which are industrially formed as by-products, as raw materials. *J. Biosci. Bioeng.* **130**, 71–75 (2020).
31. Sonoki, T. et al. Enhancement of protocatechuate decarboxylase activity for the effective production of muconate from lignin-related aromatic compounds. *J. Biotechnol.* **192**, 71–77 (2014).
32. Johnson, C. W. et al. Enhancing muconic acid production from glucose and lignin-derived aromatic compounds via increased protocatechuate decarboxylase activity. *Metab. Eng. Commun.* **3**, 111–119 (2016).
33. Salvachúa, D. et al. Bioprocess development for muconic acid production from aromatic compounds and lignin. *Green Chem.* **20**, 5007–5019 (2018).
34. Kovaleva, E. G. & Lipscomb, J. D. Versatility of biological non-heme Fe(II) centers in oxygen activation reactions. *Nat. Chem. Biol.* **4**, 186–193 (2008).
35. Mishina, Y. & He, C. Oxidative dealkylation DNA repair mediated by the mononuclear non-heme iron AlkB proteins. *J. Inorg. Biochem.* **100**, 670–678 (2006).
36. Michalak, E. M., Burr, M. L., Bannister, A. J. & Dawson, M. A. The roles of DNA, RNA and histone methylation in ageing and cancer. *Nat. Rev. Mol. Cell Biol.* **20**, 573–589 (2019).
37. Ferraro, D. J., Gakhar, L. & Ramaswamy, S. Rieske business: structure-function of Rieske non-heme oxygenases. *Biochem. Biophys. Res. Commun.* **338**, 175–190 (2005).
38. Kweon, O. et al. A new classification system for bacterial Rieske non-heme iron aromatic ring-hydroxylating oxygenases. *BMC Biochem.* **9**, 11 (2008).
39. Hannemann, F., Bichet, A., Ewen, K. M. & Bernhardt, R. Cytochrome P450 systems—biological variations of electron transport chains. *Biochim. Biophys. Acta* **1770**, 330–344 (2007).
40. Masai, E. et al. A novel tetrahydrofolate-dependent *O*-demethylase gene is essential for growth of *Sphingomonas paucimobilis* SYK-6 with syringate. *J. Bacteriol.* **186**, 2757–2765 (2004).
41. Abe, T., Masai, E., Miyauchi, K., Katayama, Y. & Fukuda, M. A tetrahydrofolate-dependent *O*-demethylase, LigM, is crucial for catabolism of vanillate and syringate in *Sphingomonas paucimobilis* SYK-6. *J. Bacteriol.* **187**, 2030–2037 (2005).
42. Jung, S. T., Lauchli, R. & Arnold, F. H. Cytochrome P450: taming a wild type enzyme. *Curr. Opin. Biotechnol.* **22**, 809–817 (2011).
43. McIntosh, J. A., Farwell, C. C. & Arnold, F. H. Expanding P450 catalytic reaction space through evolution and engineering. *Curr. Opin. Biotechnol.* **19**, 126–134 (2014).
44. Nikel, P. I. & de Lorenzo, V. *Pseudomonas putida* as a functional chassis for industrial biocatalysis: from native biochemistry to trans-metabolism. *Metab. Eng.* **50**, 142–155 (2018).
A detailed review of key metabolic pathways in *Pseudomonas putida* and analysis of the potential to leverage both native biochemistry and trans-metabolism for conversion of alternative feedstocks to valuable products in this chassis.
45. Brunel, F. & Davison, J. Cloning and sequencing of *Pseudomonas* genes encoding vanillate demethylase. *J. Bacteriol.* **170**, 4924–4930 (1988).
46. Buswell, J. A. & Ribbons, D. W. Vanillate *O*-demethylase from *Pseudomonas* species. *Method. Enzymol.* **161**, 294–301 (1988).
47. Notonier, S. et al. Metabolism of syringyl lignin-derived compounds in *Pseudomonas putida* enables convergent production of 2-pyrone-4,6-dicarboxylic acid. *Metab. Eng.* **65**, 111–122 (2021).
48. Hibi, M., Sonoki, T. & Mori, H. Functional coupling between vanillate-*O*-demethylase and formaldehyde detoxification pathway. *FEMS Microbiol. Lett.* **253**, 237–242 (2005).
49. Lanfranchi, E., Trajković, M., Barta, K., de Vries, J. G. & Janssen, D. B. Exploring the selective demethylation of aryl methyl ethers with a *Pseudomonas* Rieske monooxygenase. *ChemBioChem* **20**, 118–125 (2019).
50. Lamb, D. C., Waterman, M. R., Kelly, S. L. & Guengerich, F. P. Cytochromes P450 and drug discovery. *Curr. Opin. Biotechnol.* **18**, 504–512 (2007).
51. Li, S., Du, L. & Bernhardt, R. Redox partners: function modulators of bacterial P450 enzymes. *Trends Microbiol.* **28**, 445–454 (2020).
52. Correddu, D., Di Nardo, G. & Gilardi, G. Self-sufficient class VII cytochromes P450: from full-length structure to synthetic biology applications. *Trends Biotechnol.* **39**, 1184–1207 (2021).
53. Guengerich, F. P. Rate-limiting steps in cytochrome P450 catalysis. *Biol. Chem.* **383**, 1553–1564 (2002).
54. Eltis, L. D., Karlson, U. & Timmis, K. N. Purification and characterization of cytochrome P450RR1 from *Rhodococcus rhodochrous*. *Eur. J. Biochem.* **213**, 211–216 (1993).
55. Karlson, U. et al. Two independently regulated cytochromes P-450 in a *Rhodococcus rhodochrous* strain that degrades 2-ethoxyphenol and 4-methoxybenzoate. *J. Bacteriol.* **175**, 1467–1474 (1993).
56. Bell, S. G. et al. Cytochrome P450 enzymes from the metabolically diverse bacterium *Rhodopseudomonas palustris*. *Biochem. Biophys. Res. Commun.* **342**, 191–196 (2006).

57. Bell, S. G. et al. Crystal structure of CYP199A2, a para-substituted benzoic acid oxidizing cytochrome P450 from *Rhodopseudomonas palustris*. *J. Mol. Biol.* **383**, 561–574 (2008).
58. Tumen-Velasquez, M. et al. Accelerating pathway evolution by increasing the gene dosage of chromosomal segments. *Proc. Natl Acad. Sci. USA* **115**, 7105–7110 (2018).
59. Mallinson, S. J. B. et al. A promiscuous cytochrome P450 aromatic *O*-demethylase for lignin bioconversion. *Nat. Commun.* **9**, 2487 (2018).
60. Machovina, M. M. et al. Enabling microbial syringol conversion through structure-guided protein engineering. *Proc. Natl Acad. Sci. USA* **116**, 13970–13976 (2019).
61. Ellis, E. S. et al. Engineering a cytochrome P450 for demethylation of lignin-derived aromatic aldehydes. *JACS Au* **1**, 252–261 (2021).
Structure-guided mutagenesis converts GcoA, a guaiacol *O*-demethylase, into an efficient catalyst toward aromatic aldehydes *o*- and *p*-vanillin.
62. Fetherolf, M. M. et al. Characterization of alkylguaiacol-degrading cytochromes P450 for the biocatalytic valorization of lignin. *Proc. Natl Acad. Sci. USA* **117**, 25771–25778 (2020).
Cytochromes P450 from two Rhodococcus species catalyze the O-demethylation of lignin-derived.
63. Nelson, D. R. Cytochrome P450 diversity in the tree of life. *Biochim. Biophys. Acta* **1866**, 141–154 (2018).
64. Kawahara, N. et al. Purification and characterization of 2-ethoxyphenol-induced cytochrome P450 from *Corynebacterium* sp. strain EP1. *Can. J. Microbiol.* **45**, 833–839 (1999).
65. Sutherland, J. B. Demethylation of veratrole by cytochrome P-450 in *Streptomyces setonii*. *Appl. Environ. Microbiol.* **52**, 98–100 (1986).
66. Sauret-Ignazi, G., Dardas, A. & Pelmont, J. Purification and properties of cytochrome P-450 from *Moraxella* sp. *Biochimie* **70**, 1385–1395 (1988).
67. García-Hidalgo, J., Ravi, K., Kuré, L.-L., Lidén, G. & Gorwa-Grauslund, M. Identification of the two-component guaiacol demethylase system from *Rhodococcus rhodochrous* and expression in *Pseudomonas putida* EM42 for guaiacol assimilation. *AMB Express* **9**, 34 (2019).
68. Klenk, J. M., Ertl, J., Rapp, L., Fischer, M.-P. & Hauer, B. Expression and characterization of the benzoic acid hydroxylase CYP199A25 from *Arthrobacter* sp. *Mol. Catal.* **484**, 110739 (2020).
69. Jiang, Y. et al. Regioselective aromatic *O*-demethylation with an artificial P450BM3 peroxygenase system. *Catal. Sci. Technol.* **10**, 1219–1223 (2020).
70. Zhang, Z., Wang, Y., Zheng, P. & Sun, J. Promoting lignin valorization by coping with toxic C1 byproducts. *Trends Biotechnol.* **39**, 331–335 (2020).
71. Dev, I. K. & Harvey, R. J. Sources of one-carbon units in the folate pathway of *Escherichia coli*. *J. Biol. Chem.* **257**, 1980–1986 (1982).
72. Sonoki, T. et al. Tetrahydrofolate-dependent vanillate and syringate *O*-demethylation links tightly to one-carbon metabolic pathway associated with amino acid synthesis and DNA methylation in the lignin metabolism of *Sphingomonas paucimobilis* SYK-6. *J. Wood Sci.* **48**, 434–439 (2002).
73. Harada, A. et al. The crystal structure of a new *O*-demethylase from *Sphingobium* sp. strain SYK-6. *FEBS J.* **284**, 1855–1867 (2017).
74. Kohler, A. C., Mills, M. J. L., Adams, P. D., Simmons, B. A. & Sale, K. L. Structure of aryl *O*-demethylase offers molecular insight into a catalytic tyrosine-dependent mechanism. *Proc. Natl Acad. Sci. USA* **114**, E3205–E3214 (2017).
75. Perez, J. M. et al. Redundancy in aromatic *O*-demethylation and ring opening reactions in *Novosphingobium aromaticivorans* and their impact in the metabolism of plant derived phenolics. *Appl. Environ. Microbiol.* **87**, e02794-20 (2021).
76. Berman, M. H. & Frazer, A. C. Importance of tetrahydrofolate and ATP in the anaerobic *O*-demethylation reaction for phenylmethylethers. *Appl. Environ. Microbiol.* **58**, 925–931 (1992).
77. Kaufmann, F., Wohlfarth, G. & Diekert, G. Isolation of *O*-demethylase, an ether-cleaving enzyme system of the homoacetogenic strain MC. *Arch. Microbiol.* **168**, 136–142 (1997).
78. Naidu, D. & Ragsdale, S. W. Characterization of a three-component vanillate *O*-demethylase from *Moorella thermoacetica*. *J. Bacteriol.* **183**, 3276–3281 (2001).
79. Studenik, S., Vogel, M. & Diekert, G. Characterization of an *O*-demethylase of *Desulfitobacterium hafniense* DCB-2. *J. Bacteriol.* **194**, 3317–3326 (2012).
80. Ralph, J., Lapierre, C. & Boerjan, W. Lignin structure and its engineering. *Curr. Opin. Biotechnol.* **56**, 240–249 (2019).
81. Chenprakhon, P., Wongnate, T. & Chaiyen, P. Monooxygenation of aromatic compounds by flavin-dependent monooxygenases. *Prot. Sci.* **28**, 8–29 (2019).
Provides a comprehensive review of FMO mechanisms and structures for aromatic hydroxylation.
82. Peng, R.-H. et al. in *Reviews of Environmental Contamination and Toxicology* (ed. Whitacre, D. M.) 65–94 (Springer, 2010).
83. Ingraham, L. L. & Meyer, D. L. in *Biochemistry of Dioxygen Vol. 4 Biochemistry of the Elements* 175–178 (Springer, 1985).
84. Fitzpatrick, P. F. Mechanism of aromatic amino acid hydroxylation. *Biochemistry* **42**, 14083–14091 (2003).
85. Lah, L. et al. The versatility of the fungal cytochrome P450 monooxygenase system is instrumental in xenobiotic detoxification. *Mol. Microbiol.* **81**, 1374–1389 (2011).
86. Alber, A. & Ehlting, J. Cytochrome P450s in lignin biosynthesis. *Adv. Bot. Res.* **61**, 113–143 (2012).
87. Tinberg, C. E., Song, W. J., Izzo, V. & Lippard, S. J. Multiple roles of component proteins in bacterial multicomponent monooxygenases: phenol hydroxylase and toluene/o-xylene monooxygenase from *Pseudomonas* sp. OX1. *Biochemistry* **50**, 1788–1798 (2011).
88. Balashova, N. V. et al. Purification and characterization of a salicylate hydroxylase involved in 1-hydroxy-2-naphthoic acid hydroxylation from the naphthalene and phenanthrene-degrading bacterial strain *Pseudomonas putida* BS202-P1. *Biodegradation* **12**, 179–188 (2001).
89. Bosch, R., Moore, E. R., García-Valdés, E. & Pieper, D. H. NahW, a novel, inducible salicylate hydroxylase involved in mineralization of naphthalene by *Pseudomonas stutzeri* AN10. *J. Bacteriol.* **181**, 2315–2322 (1999).
90. Furukawa, K., Suenaga, H. & Goto, M. Biphenyl dioxygenases: functional versatilities and directed evolution. *J. Bacteriol.* **186**, 5189–5196 (2004).
91. Neidle, E. L. et al. Nucleotide sequences of the *Acinetobacter calcoaceticus benABC* genes for benzoate 1,2-dioxygenase reveal evolutionary relationships among multicomponent oxygenases. *J. Bacteriol.* **173**, 5385–5395 (1991).
92. Entsch, B. & van Berkel, W. J. Structure and mechanism of *para*-hydroxybenzoate hydroxylase. *FASEB J.* **9**, 476–483 (1995).
Pioneering investigation of aromatic hydroxylation that is still the foundation of studies published today.
93. Eppink, M. H., Overkamp, K. M., Schreuder, H. A. & Van Berkel, W. J. Switch of coenzyme specificity of *p*-hydroxybenzoate hydroxylase. *J. Mol. Biol.* **292**, 87–96 (1999).
94. Huang, Y., Zhao, K. X., Shen, X. H., Jiang, C. Y. & Liu, S. J. Genetic and biochemical characterization of a 4-hydroxybenzoate hydroxylase from *Corynebacterium glutamicum*. *Appl. Microbiol. Biotechnol.* **78**, 75–83 (2008).
95. Kasai, D. et al. Uncovering the protocatechuate 2, 3-cleavage pathway genes. *J. Bacteriol.* **191**, 6758–6768 (2009).
96. Huijbers, M. M. E., Montersino, S., Westphal, A. H., Tischler, D. & van Berkel, W. J. H. Flavin dependent monooxygenases. *Arch. Biochem. Biophys.* **544**, 2–17 (2014).
97. Chaiyen, P., Fraaije, M. W. & Mattevi, A. The enigmatic reaction of flavins with oxygen. *Trends Biochem. Sci.* **37**, 373–380 (2012).
98. Ellis, H. R. The FMN-dependent two-component monooxygenase systems. *Arch. Biochem. Biophys.* **497**, 1–12 (2010).
99. Sucharitakul, J., Chaiyen, P., Entsch, B. & Ballou, D. P. The reductase of *p*-hydroxyphenylacetate 3-hydroxylase from *Acinetobacter baumannii* requires *p*-hydroxyphenylacetate for effective catalysis. *Biochemistry* **44**, 10434–10442 (2005).
100. Palfey, B. A. & McDonald, C. A. Control of catalysis in flavin-dependent monooxygenases. *Arch. Biochem. Biophys.* **493**, 26–36 (2010).
101. Duffner, F. M., Kirchner, U., Bauer, M. P. & Müller, R. Phenol/cresol degradation by the thermophilic *Bacillus thermoglucosidasius* A7: cloning and sequence analysis of five genes involved in the pathway. *Gene* **256**, 215–221 (2000).
102. Levy-Booth, D. J. et al. Catabolism of alkylphenols in *Rhodococcus* via a *meta*-cleavage pathway associated with genomic islands. *Front. Microbiol.* **10**, 1862 (2019).
103. Sucharitakul, J., Chaiyen, P., Entsch, B. & Ballou, D. P. Kinetic mechanisms of the oxygenase from a two-component enzyme, *p*-hydroxyphenylacetate 3-hydroxylase from *Acinetobacter baumannii*. *J. Biol. Chem.* **281**, 17044–17053 (2006).
104. Hirayama, H. et al. Variation of the contents of biphenyl structures in lignins among wood species. *Holzforschung* **73**, 569–578 (2019).
105. Kumamaru, T., Suenaga, H., Mitsuoka, M., Watanabe, T. & Furukawa, K. Enhanced degradation of polychlorinated biphenyls by directed evolution of biphenyl dioxygenase. *Nat. Biotechnol.* **16**, 663–666 (1998).
106. Rogers, M. S. & Lipscomb, J. D. Salicylate 5-hydroxylase: intermediates in aromatic hydroxylation by a Rieske monooxygenase. *Biochemistry* **58**, 5305–5319 (2019).
107. Fang, T. & Zhou, N.-Y. Purification and characterization of salicylate 5-hydroxylase, a three-component monooxygenase from *Ralstonia* sp. strain U2. *Appl. Microbiol. Biotechnol.* **98**, 671–679 (2014).
108. Parales, R. E. et al. Substrate specificity of naphthalene dioxygenase: effect of specific amino acids at the active site of the enzyme. *J. Bacteriol.* **182**, 1641–1649 (2000).
109. Gally, C., Nestl, B. M. & Hauer, B. Engineering Rieske non-heme iron oxygenases for the asymmetric dihydroxylation of alkenes. *Angew. Chem. Int. Ed.* **54**, 12952–12956 (2015).
110. Ferraro, D. J., Okerlund, A., Brown, E. & Ramaswamy, S. One enzyme, many reactions: structural basis for the various reactions catalyzed by naphthalene 1,2-dioxygenase. *IUCrJ* **4**, 648–656 (2017).

111. Jouanneau, Y., Micoud, J. & Meyer, C. Purification and characterization of a three-component salicylate 1-hydroxylase from *Sphingomonas* sp. strain CHY-1. *Appl. Environ. Microbiol.* **73**, 7515–7521 (2007).
112. del Cerro, C. et al. Intracellular pathways for lignin catabolism in white-rot fungi. *Proc. Natl Acad. Sci. USA* **118**, e2017381118 (2021).
113. Seibert, C. M. & Raushel, F. M. Structural and catalytic diversity within the amidohydrolase superfamily. *Biochemistry* **44**, 6383–6391 (2005).
114. Li, T., Huo, L., Pulley, C. & Liu, A. Decarboxylation mechanisms in biological system. *Bioorg. Chem.* **43**, 2–14 (2012).
115. Goto, M. et al. Crystal structures of nonoxidative zinc-dependent 2,6-dihydroxybenzoate (gamma-resorcylate) decarboxylase from *Rhizobium* sp. strain MTP-10005. *J. Biol. Chem.* **281**, 34365–34373 (2006).
116. Vladimirova, A. et al. Substrate distortion and the catalytic reaction mechanism of 5-carboxyvanillate decarboxylase. *J. Am. Chem. Soc.* **138**, 826–836 (2016).
117. Sheng, X. et al. Mechanism and structure of gamma-resorcylate decarboxylase. *Biochemistry* **57**, 3167–3175 (2018).
118. Sheng, X. et al. A combined experimental-theoretical study of the LigW-catalyzed decarboxylation of 5-carboxyvanillate in the metabolic pathway for lignin degradation. *ACS Catal.* **7**, 4968–4974 (2017).
The empirical determination of the identity of the CO_2 as the reaction by product and density functional theory calculation that describes the molecular mechanism of the AHS-type decarboxylase.
119. Peng, X. et al. A second 5-carboxyvanillate decarboxylase gene, *ligW2*, is important for lignin-related biphenyl catabolism in *Sphingomonas paucimobilis* SYK-6. *Appl. Environ. Microbiol.* **71**, 5014–5021 (2005).
120. Kasai, D. et al. γ-Resorcylate catabolic-pathway genes in the soil actinomycete *Rhodococcus jostii* RHA1. *Appl. Environ. Microbiol.* **81**, 7656–7665 (2015).
121. Spence, E. M. et al. The hydroxyquinol degradation pathway in *Rhodococcus jostii* RHA1 and *Agrobacterium* species is an alternative pathway for degradation of protocatechuic acid and lignin fragments. *Appl. Environ. Microbiol.* **86**, e01561–e01520 (2020).
122. Meier, A. K. et al. Agdc1p—a gallic acid decarboxylase involved in the degradation of tannic acid in the yeast *Blastobotrys* (*Arxula*) *adeninivorans*. *Front. Microbiol.* **8**, 1777 (2017).
123. Brückner, C., Oreb, M., Kunze, G., Boles, E. & Tripp, J. An expanded enzyme toolbox for production of *cis*, *cis*-muconic acid and other shikimate pathway derivatives in *Saccharomyces cerevisiae*. *FEMS Yeast Res.* **18**, foy017 (2018).
124. Zeug, M. et al. Crystal structures of non-oxidative decarboxylases reveal a new mechanism of action with a catalytic dyad and structural twists. *Sci. Rep.* **11**, 3056 (2021).
A novel NTF2-type cofactorless gallate/protocatechuate decarboxylase from fungi.
125. White, M. D. et al. UbiX is a flavin prenyltransferase required for bacterial ubiquinone biosynthesis. *Nature* **522**, 502–506 (2015).
126. Lupa, B., Lyon, D., Gibbs, M. D., Reeves, R. A. & Wiegel, J. Distribution of genes encoding the microbial non-oxidative reversible hydroxyarylic acid decarboxylases/phenol carboxylases. *Genomics* **86**, 342–351 (2005).
127. Lupa, B., Lyon, D., Shaw, L. N., Sieprawska-Lupa, M. & Wiegel, J. Properties of the reversible nonoxidative vanillate/4-hydroxybenzoate decarboxylase from *Bacillus subtilis*. *Can. J. Microbiol.* **54**, 75–81 (2008).
128. Payne, K. A. et al. New cofactor supports α,β-unsaturated acid decarboxylation via 1,3-dipolar cycloaddition. *Nature* **522**, 497–501 (2015).
129. Wang, P. H. et al. Biosynthesis and activity of prenylated FMN cofactors. *Cell Chem. Biol.* **25**, 560–570 (2018).
130. Walsh, C. T. & Wencewicz, T. A. Flavoenzymes: versatile catalysts in biosynthetic pathways. *Nat. Prod. Rep.* **30**, 175–200 (2013).
131. Payer, S. E. et al. Regioselective *para*-carboxylation of catechols with a prenylated flavin dependent decarboxylase. *Angew. Chem. Int. Ed.* **56**, 13893–13897 (2017).
Structural and catalytic properties of the UbiD-type decarboxylase.
132. Grant, D. J. & Patel, J. C. The non-oxidative decarboxylation of *p*-hydroxybenzoic acid, gentisic acid, protocatechuic acid and gallic acid by *Klebsiella aerogenes* (*Aerobacter aerogenes*). *Antonie Van Leeuwenhoek* **35**, 325–343 (1969).
133. Matsui, T., Yoshida, T., Hayashi, T. & Nagasawa, T. Purification, characterization, and gene cloning of 4-hydroxybenzoate decarboxylase of *Enterobacter cloacae* P240. *Arch. Microbiol.* **186**, 21–29 (2006).
134. Holesova, Z. et al. Gentisate and 3-oxoadipate pathways in the yeast *Candida parapsilosis*: identification and functional analysis of the genes coding for 3-hydroxybenzoate 6-hydroxylase and 4-hydroxybenzoate 1-hydroxylase. *Microbiology* **157**, 2152–2163 (2011).
135. Katagiri, M., Takemori, S., Suzuki, K. & Yasuda, H. Mechanism of the salicylate hydroxylase reaction. *J. Biol. Chem.* **241**, 5675–5677 (1966).
136. Reiner, A. M. Metabolism of aromatic compounds in bacteria. Purification and properties of the catechol-forming enzyme, 3,5-cyclohexadiene-1,2-diol-1-carboxylic acid (NAD^+) oxidoreductase (decarboxylating). *J. Biol. Chem.* **247**, 4960–4965 (1972).
137. Neidle, E. et al. *Cis*-diol dehydrogenases encoded by the TOL pWW0 plasmid *xylL* gene and the *Acinetobacter calcoaceticus* chromosomal *benD* gene are members of the short-chain alcohol dehydrogenase superfamily. *Eur. J. Biochem.* **204**, 113–120 (1992).
138. Reiner, A. M. Metabolism of benzoic acid by bacteria: 3,5-cyclohexadiene-1,2-diol-1-carboxylic acid is an intermediate in the formation of catechol. *J. Bacteriol.* **108**, 89–94 (1971).
139. Cho, O. et al. Catabolic role of a three-component salicylate oxygenase from *Sphingomonas yanoikuyae* B1 in polycyclic aromatic hydrocarbon degradation. *Biochem. Biophys. Res. Commun.* **327**, 656–662 (2005).
140. Becker, J. & Wittmann, C. Advanced biotechnology: metabolically engineered cells for the bio-based production of chemicals and fuels, materials and health-care products. *Angew. Chem. Int. Ed.* **54**, 3328–3350 (2015).
141. Kuatsjah, E. et al. Debottlenecking 4-hydroxybenzoate hydroxylation in *Pseudomonas putida* KT2440 improves muconate productivity from p-coumarate. *Metab. Eng.* **70**, 31–42 (2021).
142. Zobel, S., Kuepper, J., Ebert, B., Wierckx, N. & Blank, L. M. Metabolic response of *Pseudomonas putida* to increased NADH regeneration rates. *Eng. Life Sci.* **17**, 47–57 (2017).
143. Lubbers, R. J. M. et al. Discovery of novel *p*-hydroxybenzoate-*m*-hydroxylase, protocatechuate 3,4 ring-cleavage dioxygenase, and hydroxyquinol 1,2 ring-cleavage dioxygenase from the filamentous fungus *Aspergillus niger*. *ACS Sustain. Chem. Eng.* **7**, 19081–19089 (2019).
144. Wang, M., Chen, B., Fang, Y. & Tan, T. Cofactor engineering for more efficient production of chemicals and biofuels. *Biotechnol. Adv.* **35**, 1032–1039 (2017).
145. Bell, S. G., Tan, A. B., Johnson, E. O. & Wong, L.-L. Selective oxidative demethylation of veratric acid to vanillic acid by CYP199A4 from *Rhodopseudomonas palustris* HaA2. *Mol. Biosyst.* **6**, 206–214 (2009).
146. Khatri, Y., Schifrin, A. & Bernhardt, R. Investigating the effect of available redox protein ratios for the conversion of a steroid by a myxobacterial CYP 260A1. *FEBS Lett.* **591**, 1126–1140 (2017).
147. To, P., Whitehead, B., Tarbox, H. E. & Fried, S. D. Nonrefoldability is pervasive across the *E. coli* proteome. *J. Am. Chem. Soc.* **143**, 11435–11448 (2021).
148. Zhu, Z. et al. Development of engineered ferredoxin reductase systems for the efficient hydroxylation of steroidal substrates. *ACS Sustain. Chem. Eng.* **8**, 16720–16730 (2020).
149. Zhang, W. et al. New reactions and products resulting from alternative interactions between the p450 enzyme and redox partners. *J. Am. Chem. Soc.* **136**, 3640–3646 (2014).
150. Chen, N. H., Djoko, K. Y., Veyrier, F. J. & McEwan, A. G. Formaldehyde stress responses in bacterial pathogens. *Front. Microbiol.* **7**, 257 (2016).
151. Nguyen, L. T., Tran, M. H. & Lee, E. Y. Co-upgrading of ethanol-assisted depolymerized lignin: a new biological lignin valorization approach for the production of protocatechuic acid and polyhydroxyalkanoic acid. *Bioresour. Technol.* **338**, 125563 (2021).
152. Sandberg, T. E., Salazar, M. J., Weng, L. L., Palsson, B. O. & Feist, A. M. The emergence of adaptive laboratory evolution as an efficient tool for biological discovery and industrial biotechnology. *Metab. Eng.* **56**, 1–16 (2019).
A comprehensive review of adaptive laboratory evolution principles, applications and potential to optimize relevant features of industrial microbial chassis.
153. Mohamed, E. T. et al. Adaptive laboratory evolution of *Pseudomonas putida* KT2440 improves *p*-coumaric and ferulic acid catabolism and tolerance. *Metab. Eng. Commun.* **11**, e00143 (2020).
154. Salvachúa, D. et al. Outer membrane vesicles catabolize lignin-derived aromatic compounds in *Pseudomonas putida* KT2440. *Proc. Natl Acad. Sci. USA* **117**, 9302–9310 (2020).
155. Alves, N. J. et al. Bacterial nanobioreactors—directing enzyme packaging into bacterial outer membrane vesicles. *ACS Appl. Mater. Interfaces* **7**, 24963–24972 (2015).
156. Elmore, J. R. et al. Production of itaconic acid from alkali pretreated lignin by dynamic two stage bioconversion. *Nat. Commun.* **12**, 2261 (2021).
157. Foo, J. L., Ching, C. B., Chang, M. W. & Leong, S. S. J. The imminent role of protein engineering in synthetic biology. *Biotechnol. Adv.* **30**, 541–549 (2012).
158. Maxel, S. et al. A growth-based, high-throughput selection platform enables remodeling of 4-hydroxybenzoate hydroxylase active site. *ACS Catal.* **10**, 6969–6974 (2020).
159. Jha, R. K. et al. A protocatechuate biosensor for *Pseudomonas putida* KT2440 via promoter and protein evolution. *Metab. Eng. Commun.* **6**, 33–38 (2018).
160. Wiechert, W. ^{13}C metabolic flux analysis. *Metab. Eng.* **3**, 195–206 (2001).
161. Vermaas, J. V. et al. Passive membrane transport of lignin-related compounds. *Proc. Natl Acad. Sci. USA* **116**, 23117 (2019).

162. Wada, A. et al. Characterization of aromatic acid/proton symporters in *Pseudomonas putida* KT2440 toward efficient microbial conversion of lignin-related aromatics. *Metab. Eng.* **64**, 167–179 (2021).
163. Conrado, R. J., Varner, J. D. & DeLisa, M. P. Engineering the spatial organization of metabolic enzymes: mimicking nature's synergy. *Curr. Opin. Biotechnol.* **19**, 492–499 (2008).
164. Lee, H., DeLoache, W. C. & Dueber, J. E. Spatial organization of enzymes for metabolic engineering. *Metab. Eng.* **14**, 242–251 (2012).
165. Entsch, B., Cole, L. J. & Ballou, D. P. Protein dynamics and electrostatics in the function of *p*-hydroxybenzoate hydroxylase. *Arch. Biochem. Biophys.* **433**, 297–311 (2005).
A summary of the *p*-hydroxybenzoate hydroxylase catalytic cycle.
166. van Berkel, W. J. H., Kamerbeek, N. M. & Fraaije, M. W. Flavoprotein monooxygenases, a diverse class of oxidative biocatalysts. *J. Biotechnol.* **124**, 670–689 (2006).
167. Leys, D. Flavin metamorphosis: cofactor transformation through prenylation. *Curr. Opin. Chem. Biol.* **47**, 117–125 (2018).

Acknowledgements

We thank many of our colleagues for helpful discussions that informed the topics covered in this Review, including P. Abraham, R. Giannone, A. Guss, R. Hettich, C. Johnson, C. Maranas, J. Michener, E. Neidle and D. Salvachúa, among many others. This work was authored in part by the National Renewable Energy Laboratory, operated by Alliance for Sustainable Energy for the US Department of Energy (DOE) under contract no. DE-AC36-08GO28308. E.E., A.B., E.K., A.Z.W. and G.T.B. are supported by The Center for Bioenergy Innovation (CBI), a US DOE Bioenergy Research Center supported by the Office of Biological and Environmental Research (BER) in the DOE Office of Science. G.T.B. also thanks the US DOE Energy Efficiency and Renewable Energy (EERE) Bioenergy Technologies Office (BETO). L.D.E. is the recipient of a Canada Research Chair. L.D.E.'s research on lignin has been supported by the Natural Sciences and Engineering Research Council of Canada (NSERC), Genome BC and Genome Canada. J.E.M. acknowledges Research England for E3 funding. The views expressed in the Review do not necessarily represent the views of the DOE or the US Government. The US Government retains and the publisher, by accepting the Article for publication, acknowledges that the US Government retains a non-exclusive, paid-up, irrevocable, worldwide license to publish or reproduce the published form of this work, or allows others to do so, for US Government purposes.

Author contributions

E.E., A.B., E.K., A.Z.W., J.L.D., J.E.M., L.D.E. and G.T.B. wrote the manuscript and designed the figures. All authors edited the manuscript before submission.

Competing interests

The authors declare no competing interests.

Additional information

Supplementary information The online version contains supplementary material available at https://doi.org/10.1038/s41929-022-00747-w.

Correspondence should be addressed to Lindsay D. Eltis or Gregg T. Beckham.

Peer review information *Nature Catalysis* thanks the anonymous reviewers for their contribution to the peer review of this work.

Reprints and permissions information is available at www.nature.com/reprints.

Publisher's note Springer Nature remains neutral with regard to jurisdictional claims in published maps and institutional affiliations.